Available online at www.sciencedirect.com
SCIENCE DIRECT®
PERGAMON
International Journal of Heat and Mass Transfer 46 (2003) 4345–4349
International Journal of HEAT and MASS TRANSFER
www.elsevier.com/locate/ijhmt

Technical Note

The internal surface area basis, a key issue of modeling fouling in enhanced heat transfer tubes

Wei Li

Breezy Tree Court, Apt. 2H, Timonium, MD 21093, USA

Received 18 October 2002; received in revised form 28 April 2003

Abstract

The purpose of this paper is to discuss the internal surface area basis, a key issue of modeling fouling in enhanced heat transfer tubes, and to correct an *error* in the author's previous paper, Li and Webb [Int. J. Heat Mass Transfer 45 (2002) 1685]. A fouling factor can be defined based on one of the two area bases, nominal internal surface area and total internal surface area. The error was originated from incorrect definition of internal surface area basis.

Keywords: Fouling; Cooling tower; Enhanced tube; Turbulent flow

1. Introduction

The two subject areas of fouling and enhancement have been developed mainly independently for many years. Watkinson [1] had attempted to bring the two areas together in an early paper. Chamra and Webb [2] tested accelerated particulate fouling behavior for a wide range of particle size distribution and foulant concentration for two different types of in-tube enhancements and a smooth tube. Rabas et al. [3] monitored the fouling characteristics of helically corrugated (indented) steam condenser tubes in an electric utility plant for 15 months. Bott [4] and Epstein [5] described information on particle deposition. Webb [6], and Somerscales and Bergles [7] summarized much of the relevant prior work on accelerated fouling in enhanced tubes.

Webb and Li [8] provided the data on long-term fouling in practical situations. The tests were conducted in seven 15.54 mm ID copper, helically ribbed tubes as shown in Table 1 using cooling tower water. Li and Webb [9] further provided correlations of the experimental results of Webb and Li [8] to quantitatively define the effect of rib height, rib axial pitch, and helix angle on the tube fouling performance. Even though the correlations can be directly used to assess the fouling potential of enhanced tubes in actual cooling water situations, there is an *error* in the Section 3.2 of Li and Webb [9], bordering on a misinformation of potential readers including a number of wrong or misleading statements. It was originated from incorrect definition of internal surface area basis. The purpose of this paper is to discuss the internal surface area basis, a key issue of modeling fouling in enhanced heat transfer tubes, and to correct the error in the author's previous paper.

1.1. Two area bases

We can define the fouling factor on two area bases. They are: R_f, based on nominal area, and R_{ft}, based on total internal area. The overall thermal resistance $(1/UA)$ is given by

$$\frac{1}{UA}=\frac{1}{h_i A_i}+\frac{R_f}{A_i}+\frac{1}{h_o A_o}=R_i+R_{foul}+R_o \tag{1}$$

One must specify the area basis for the fouling factor in Eq. (1), using either of the definitions given above. One may convert from R_f definition to R_{ft} definition using the following relationship,

$$R_{foul}=\frac{R_f}{A_p}=\frac{R_{ft}}{A_t} \tag{2}$$

E-mail address: weili96@hotmail.com (W. Li).

0017-9310/$ - see front matter
doi:10.1016/S0017-9310(03)00254-0

Nomenclature

A	surface area, m^2
A_c	cross-sectional area, m^2
D_i	internal tube diameter, or diameter to root of fins, m
f	friction factor, dimensionless
G	mass velocity ($=\dot{m}/A_c$), kgm^{-2}
h	heat transfer coefficient, $W\,m^{-2}$
j	Colburn j-factor ($=StPr^{2/3}$), dimensionless
L	tube length, m
$\dot{m}$	mass flow rate, $kg\,s^{-1}$
ΔP	tube side pressure drop, N/m^2
Pr	Prandtl number, dimensionless
St	Stanton number, dimensionless
R_f	fouling factor based on nominal area, m^2 K/W
R_f^*	asymptotic fouling factor based on nominal area, m^2 K/W
R_{foul}	fouling thermal resistance per square area ($=R_f/A$), K/W
U	overall heat transfer coefficient, W/m^2 K

Greek symbols

β	area index, $(A_t/A_{tp})/(A_c/A_{cp})$, dimensionless
η	efficiency index, $(j/j_p)/(f/f_p)$, dimensionless
σ	fouling process index, dimensionless
ρ	fluid density, kg/m^3
τ_w	wall shear stress, N/m^2

Subscripts

i	inside
o	outside
p	plain surface
t	total internal area

Table 1
Experimental fouling ratio and experimental heat transfer enhancement ratio (referred to plain tube)

Tube	R_{ft}/R_{fp}	R_f/R_{fp}	η	β	A_c/A_{cp}	A_t/A_p	h/h_p
2	8.19	5.15	1.18	1.66	0.96	1.59	2.32
5	5.61	3.40	1.04	1.75	0.94	1.65	2.26
3	3.45	2.26	1.05	1.56	0.95	1.48	2.33
6	2.25	1.57	1.01	1.52	0.94	1.43	2.08
7	2.14	1.51	1.05	1.52	0.94	1.42	1.93
8	1.64	1.25	0.98	1.40	0.94	1.31	1.51
4	1.32	1.13	0.95	1.24	0.94	1.17	1.74
1	1.0	1.0	1.0	1.0	1.0	1.0	1.0

$D_i = 15.54$ mm, $R_{fp} = 2.8E{-}5$ m^2 K/W, $h_p = 6730$ W/m^2 K, $f_p = 0.0257$.

The ARI allows equipment manufacturers to include a "design fouling factor" in Eq. (1) for the machine design rating. The logic of this is that when the machine was tested in the laboratory, no fouling occurred over the short (e.g., two weeks) test period. Hence one "rates" the machine for operating conditions expected to occur in seasonal operation. The R_{ARI} value specified by ARI is $4.4E{-}5$ m^2 K/W (2.5 E−4 h ft^2 °F/Btu). This value currently applies to all internal tube geometries. For the case of "internally enhanced" tubes, which have larger internal surface area than a plain tube, one must decide whether to use the actual, total internal surface area, or whether to use the "nominal" plain tube area ($A_p = \pi D_i L$) in Eq. (1). Equipment manufacturers choose to use the actual, total internal surface area. An important implication of this is that it will result in a smaller de-rating of the unit. This is illustrated for Tube 2, which has $A_t/A_p = 1.59$, as shown in Table 1. If we write the UA-value on a "per unit length" basis, the fouling thermal resistance is $R_{ARI}(L/A_i)$. Hence the fouling thermal resistance added for Tube 2 depends on the area basis applied to the fouling factor. It is calculated below for each of the possible area definitions.

$R_{ARI}(L/A_t)$ based on total internal surface area:

$$R_{ARI}\left(\frac{L}{A_t}\right) = R_{ARI}\left(\frac{1}{1.59\pi D_i}\right) = 2.07E-3\ \text{m K/W} \quad (3)$$

$R_{ARI}(L/A_p)$ based on nominal internal surface area:

$$R_{ARI}\left(\frac{L}{A_p}\right) = R_{ARI}\left(\frac{1}{\pi D_i}\right) = 3.29E-3\ \text{m K/W} \quad (4)$$

Although the $R_{ARI}(L/A_t)$ and $R_{ARI}(L/A_p)$ may seem like a small number, one must measure it relative to the "water side convection thermal resistance", L/h_iA_i. As

shown by Eq. (1), the fouling thermal resistance (R_{foul}) is added to the convection thermal resistance ($1/h_iA_i$). For Tube 2, $L/h_iA_i = 11.1E{-}3\ m^2\,K/W$. The sum ($1/h_iA_i + R_{foul}$) is the total water side thermal resistance ($R_{i,tot}$). If R_{foul} is based on the "total internal surface area", the addition of R_{ARI} increases $R_{i,tot}$ by 19% [100(11.1 + 2.07)/11.1]. However, if R_{foul} is based on the "nominal internal surface area", the resistance increase would be 30% [100(11 + 3.29)/11.1]. The next question of importance is—What is the magnitude of the total water side thermal resistance for the measured fouling factors obtained from the fouling tests? As shown by column 1 of Table 1, the highest measured R_{ft} is $22.9E{-}5\ m^2\,K/W$. This value is 5.21 times larger than the R_{ARI}. Such a fouling resistance would result in a very large increase of the total water side thermal resistance. For Tube 2, the $R_{i,tot}$ increase would be 197% [100(11.1 + 5.21 × 2.07)/11.1].

2. Fouling data analysis

2.1. An error in Li and Webb [9]

We would like to quote the Section 3.2 in Li and Webb [9]:

$$\frac{R_f^*}{R_{fp}^*} \propto \frac{j/j_p}{\tau_w/\tau_{wp}} \tag{5}$$

Because the $e/D_i < 0.04$ of the tubes investigated in this study is small, the momentum in the axial direction is much larger than the angular momentum promoted by the ribs. The apparent shear stress, obtained from pressure drop data, is used to approximate the wall shear stress (τ_{wt}). The τ_{wt} is given by

$$\Delta P A_c = \tau_{wt} A_t \tag{6}$$

Combining Eqs. (5) and (6):

$$\frac{R_f^*}{R_{fp}^*} \propto \beta\eta \tag{7}$$

$\beta = (A_t/A_p)/(A_c/A_{cp})$ is an area index and $\eta = (j/j_p)/(f/f_p)$ is the efficiency index, where f is the friction factor and j is the Colburn j-factor. β and η are normally provided by the tube manufacturers. As previously noted, the R_f^*, f, and j are based on the nominal surface area. By correlating R_f/R_{fp}, fouling factor ratios at the end of one cooling season, with $\beta\cdot\eta$ in Table 1 using Eq. (7). Li and Webb [9] obtained the following correlations:

$$\frac{R_f}{R_{fp}} = \beta\eta \quad 10.0 > p/e \geqslant 5.0 \tag{8a}$$

$$\frac{R_f}{R_{fp}} = 0.178(\beta\eta)^{5.03} \quad p/e < 5.0 \tag{8b}$$

Eqs. (8a) and (8b) have an average deviation of 4.5%. They can be directly used to assess the fouling potential of enhanced tubes in actual cooling water situations.

There is an error in the above analysis. Please note that the R_f^* and τ_w in Eq. (5) must be defined on the same area basis. Because the R_f^*/R_{fp}^* is based on A_p, one must use the same A_p for τ_w. However, τ_{wt} is based on A_t as shown in Eq. (6). Therefore, Eq. (7) is not valid because Eq. (5) is based on A_p and Eq. (6) is based on A_t. The correct analysis is as following: by definition,

$$\tau_w = f(G^2/2\rho) \tag{9}$$

Setting $G =$ constant and substituting Eq. (9) into Eq. (5) give:

$$\frac{R_f^*}{R_{fp}^*} = \sigma_p\eta \tag{10}$$

σ_p is a fouling process index based on A_p, which is determined from the fouling tests. By comparing Eq. (10) to Eq. (7), we observe that R_f^*/R_{fp}^* is proportional to η instead of $\beta\cdot\eta$.

2.2. Correlations based on the total internal surface area

The equipment manufacturers use the actual, total internal surface area. We need develop correlations of R_{ft}^*/R_{fp}^*, which is based on the total internal surface area. According to Eq. (5), we obtain the following relation:

$$\frac{R_{ft}^*}{R_{fp}^*} \propto \frac{j_t/j_p}{\tau_{wt}/\tau_{wp}} \tag{11}$$

Eq. (11) may be transformed to a different form using the following relations: $j_tA_t = j_iA_i$ and Eq. (6). Substituting these relations into Eq. (11) gives:

$$\frac{R_{ft}^*}{R_{fp}^*} = \sigma_t\eta\frac{A_{cp}}{A_c} = 0.95\sigma_t\eta \tag{12}$$

σ_t is a fouling process index based on A_t, which is determined from the fouling tests. The ratios of A_{cp}/A_c for the tested tubes in this study are between 0.94 and 0.96 as shown in Table 1. We use 0.95 for A_{cp}/A_c in Eq. (12). By comparing Eq. (10) to Eq. (12), we observe that R_{ft}^*/R_{fp}^* is also proportional to η. R_{ft}/R_{fp} shall have a similar behavior to R_f/R_{fp} according to Eqs. (10) and (12). This is confirmed by Fig. 1a. Fig. 1a also shows that R_{ft}/R_{fp} and R_f/R_{fp} are not able to be correlated by η. However, Eq. (7) correlated the experimental data well by using $\beta\cdot\eta$ as shown in Eqs. (8a) and (8b). If we correlate R_{ft}/R_{fp}, fouling factor ratios at the end of one cooling season, with $\beta\cdot\eta$ as shown in Table 1, we obtain the following correlations:

$$\frac{R_{ft}}{R_{fp}} = 2.3\beta\eta - 1.4 \quad 10.0 > p/e \geqslant 5.0 \tag{13a}$$

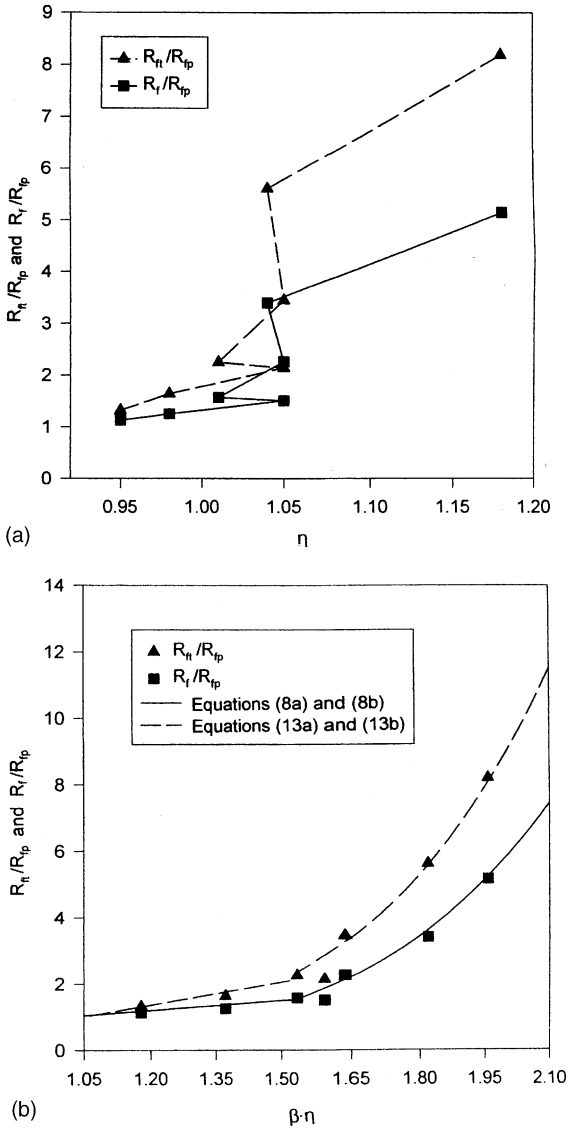

Fig. 1. (a) R_{ft}/R_{fp} and R_f/R_{fp} vs. η, (b) R_{ft}/R_{fp} and R_f/R_{fp} vs. $\beta \cdot \eta$.

$$\frac{R_{ft}}{R_{fp}} = 0.27(\beta\eta)^{5.07} \quad p/e < 5.0 \tag{13b}$$

Eqs. (13a) and (13b) have an average deviation of 6.5%.

Eqs. (10) and (12) are not able to correlate the experimental data as shown in Fig. 1a, but Eqs. (8) and (13) correlated the data well as shown in Fig. 1b. There appears to be a gab between theoretical analysis and experimental data. Little understanding exists of the role of β in the modeling process. The helical-rib tubes provided significant surface area increase, which is reflected in β.

Both particulate and precipitation fouling (P&PF) existed in cooling tower [8]. Fig. 2a shows that significant physical P&PF deposits cover the total internal surface of a tested tube 2 after the completion of tests in one cooling season. Fig. 2b shows the corresponding fouling data of the tube 2. The P&PF deposits on the total internal surface including the surfaces between ribs, rib tip surfaces, and side surfaces of ribs, due to deposit cohesion. If there is no deposit cohesion as particulate fouling, the fouling deposit will be on the surface between the ribs and on the rib tip surface only [2]. It is probable that β (or A_t/A_p) should be manually added into Eqs. (8) and (13) to include the effect of deposit cohesion. Further studies are needed to investigate the reason of adding β, the gab between theoretical analysis and experimental data.

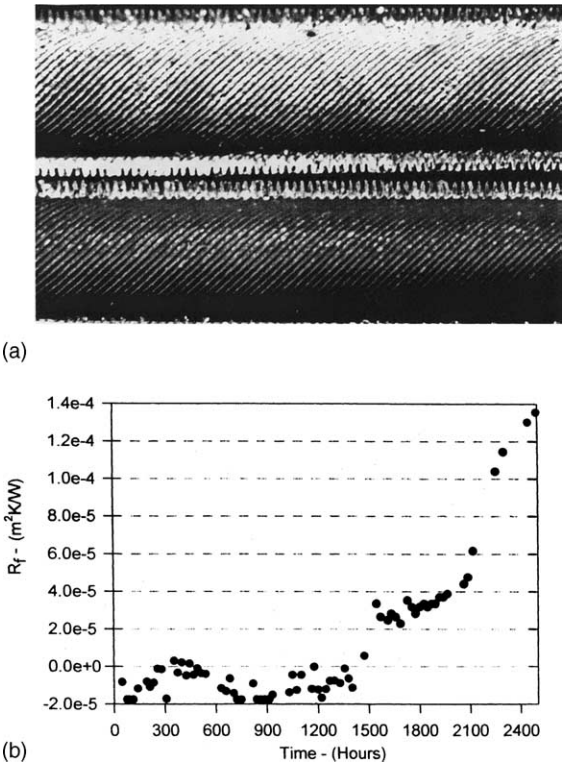

Fig. 2. (a) A photo of fouled (upper photo) and unfouled (lower photo) tube 2 after completion of P&PF test. (b) A sample of experimental P&PF data of the tube 2.

3. Conclusions

1. The purpose of this paper is to discuss the internal surface area basis, a key issue of modeling fouling in enhanced heat transfer tubes, and to correct an error in the author's previous paper, Li and Webb [9]. A fouling factor can be defined based on one of the two area bases, nominal internal surface area and total internal surface area. The error was originated from incorrect definition of internal surface area basis.

2. A series of semi-theoretical fouling correlations as a function of $\beta \cdot \eta$ based on total internal surface area was developed. The correlations can be directly used to assess the fouling potential of enhanced tubes in actual cooling water situations.

Acknowledgements

The author would like to thank Prof. Ralph L. Webb in mechanical engineering at Penn State for his valuable contributions throughout the process of writing this paper. The author would like to thank Mr. Petur Thors at Wolverine Tube for his valuable suggestion and discussion.

References

[1] A.P. Watkinson, Fouling of augmented heat transfer tubes, Heat Transfer Eng. 11 (3) (1990) 57–61.

[2] L.M. Chamra, R.L. Webb, Modeling liquid-side particulate fouling in enhanced tubes, Int. J. Heat Mass Transfer 37 (4) (1994) 571–579.

[3] T.J. Rabas et al., Comparison of power-plant condenser cooling-water fouling rates for spirally-indented and plain tubes, Fouling Enhancement Interact. HTD 164 (1991) 29–36.

[4] T.R. Bott, Fouling of Heat Exchangers, Elsevier Science, New York, 1995.

[5] N. Epstein, Elements of particle deposition onto nonporous solid surface parallel to suspension flows, Exp. Therm. Fluid Sci. 14 (4) (1997) 323–334.

[6] R.L. Webb, Principles of Enhanced Heat Transfer, first ed., Wiley Interscience, New York, 1994, pp. 285–309.

[7] E.F.C. Somerscales, A.E. Bergles, Enhancement of heat transfer and fouling mitigation, Advances in Heat Transfer, vol. 30, Academic Press, 1997, pp. 197–253.

[8] R.L. Webb, W. Li, Fouling in enhanced tubes using cooling tower water. Part I: Long term fouling data, Int. J. Heat Mass Transfer 43 (2000) 3567–3578.

[9] W. Li, R.L. Webb, Fouling characteristics of internal helical-rib roughness tubes using low-velocity cooling tower water, Int. J. Heat Mass Transfer 45 (2002) 1685–1691.